J Sol-Gel Sci Technol (2009) 50:58–68
DOI 10.1007/s10971-009-1905-6

ORIGINAL PAPER

A spectroscopic study of calcium aluminate gels obtained from aluminium *sec*-butoxide chelated with ethyl acetoacetate in various ratios

S. Kurajica · G. Mali · T. Gazivoda · J. Sipusic · V. Mandic

Received: 17 July 2008 / Accepted: 16 January 2009 / Published online: 5 February 2009

Abstract Calcium aluminate ($CaAl_2O_4$, CA) powders were prepared by sol–gel technique at low sintering temperatures. Aluminium-*sec*-butoxide ($Al(O^sBu)_3$, Asb) and calcium nitrate tetrahydrate ($Ca(NO_3)_2 \times 4H_2O$) were used as starting materials. Ethyl acetoacetate ($C_6H_{10}O_3$, Eaa) was used as a chelating agent in order to control the rate of hydrolysis of $Al(O^sBu)_3$. Three gels with Eaa/Asb molar ratios of 1/1, 3/2 and 2/1 were prepared. The dried gels and thermally treated samples were characterized by means of Fourier Transform Infrared spectroscopy (FTIR), ^1H, ^{13}C Nuclear Magnetic Resonance (NMR) spectroscopy, solid-state ^{27}Al Magic Angle Spinning (MAS) NMR, 3Q MAS NMR spectroscopy, and X-Ray Diffraction (XRD). From the results obtained, the effect of modification of the starting Asb on the hydrolysis process, hydrolyzed gel structure and crystallization behavior is discussed. It has been established that Eaa reacts completely with Asb forming chelate. Various chelate units are formed including trichelated, $Al(Eaa)_3$ units. Spontaneous gellation has been observed in the sols slowly hydrolyzed by exposing to air moisture. The reactivity towards hydrolysis of chelated alkoxide depends on the number of chelating ligands bonded to aluminium. *Sec*-butoxy groups were primarily hydrolyzed; ethyl acetoacetate groups in less chelated units are much less susceptible to hydrolysis, while trichelated units were not hydrolyzed. Thus, in hydrolyzed gels a partially chelated oligomers and trichelated $Al(Eaa)_3$ units exist. The crystal phase, not described previously, related to $Al(Eaa)_3$ chelate crystallizes in the gels with higher Eaa/Asb ratio. Hydrolysis leads to formation of three kinds of Al coordination sites: six coordinated $Al(Eaa)_3$, and five and six coordinated Al atoms in oligomers. The Eaa/Asb ratio strongly influences the relative ratios between the various coordination states of aluminium atom. After thermal treatment of the gels at 1,000 °C for 2 h, CA was obtained along with minor $CaAl_4O_7$, (CA_2) and $Ca_{12}Al_{14}O_{33}$($C_{12}A_7$) compounds. Thermal treatment at higher temperature increases the amount of CA and decreases the amount of minor components.

Keywords Calcium aluminate · Aluminium *sec*-butoxide · Ethyl acetoacetate · Sol–gel · Solid-state MAS NMR

1 Introduction

Calcium aluminate, CA, is the main crystalline phase of aluminate cement and an important refractory material. Crystalline calcium aluminate is also used in high strength and high toughness ceramic-polymer composite materials [1] and plays an important role in the processing and performance of chemically bonded ceramics [2]. Recently, new applications for calcium aluminate have emerged in optical and structural ceramics. CA glasses have small scattering losses and IR transmissions superior to most ordinary oxide glasses and thus they have possible applications as optical fibers [3]. Some CA glasses are photosensitive, which makes them potential candidates for information storage devices [3]. Recently, it has been demonstrated that CA have bioactive properties and

S. Kurajica (✉) · T. Gazivoda · J. Sipusic · V. Mandic
Faculty of Chemical Engineering and Technology, University of Zagreb, 19 Marulicev trg, Zagreb, Croatia
e-mail: stankok@fkit.hr

G. Mali
National Institute of Chemistry, 19 Hajdrihova, Ljubljana, Slovenia

CA-based materials have been investigated as bioactive dental material [4].

For advanced applications high purity CA is required. The preparation of pure CA phase is also of importance for research in cement chemistry. The use of pure CA enables deeper insight in the hydration process kinetics or the influence of minor elements and additives on the reactivity of cement [5].

The traditional technique of preparing pure calcium aluminate compounds is by solid state reactions (sintering) of calcium and aluminium oxides (or oxide precursors such as carbonates or oxalates). Precursors are physically mixed, held at high temperatures (required for solid-state diffusion process) for extended time, grinded and re-sintered. This process takes several hours up to days with several intermediate grindings [5] and still does not allow the fine control of the phase composition and the microstructure due to limitations of physical mixing to the micrometer scale, yielding multiple, unwanted phases [1]. Therefore, the advanced CA applications such as fibers, thin films and coatings require sophisticated preparation process.

Various chemical approaches have been developed for the synthesis of pure, single phase calcium aluminate powders: e.g., evaporation [1], spray-drying [2], Pechini process [6] and self-propagating high temperature synthesis (combustion synthesis) [7] and sol–gel process.

In order to provide a more efficient way for the synthesis of pure phases, the sol–gel process was introduced to synthesize amorphous calcium aluminate powders. The sol–gel method is a wet-chemical process with multiple advantages to solid state reaction methods. Such advantages had been related to good mixing of starting reagents yielding more homogeneous products with greater reactivity. Consequently, the crystallization is achieved by subsequent heating of amorphous gel and lower processing temperature.

One of the early attempts of sol–gel synthesis of calcium aluminate powders was reported by Uberoi and Risbud [8]. They used $Ca(NO_3)_2 \times 4H_2O$ and aluminium *di-sec*-butoxide acetoacetic ester chelate because the use of pure Asb as alumina source was found impracticable due to the rapid hydrolysis of Asb when exposed to air. Goktas and Weinberg [3] prepared calcium aluminate gels from $Ca(NO_3)_2 \times 4H_2O$ and Asb using HCl in dissolution procedure. Same method was adopted by Kerns et al. [9]. Aitasalo et al. [10] employed aluminium isopropoxide and $Ca(NO_3)_2 \times 4H_2O$.

Aluminium alkoxides, such as Asb, are known for their high affinity for water, uncontrolled hydrolysis of those precursors results in an aluminium hydroxide precipitate [11]. The rapid rate of hydrolysis of the alkoxide precursor is due to the presence of an electronegative alkoxy group which makes the metal atom highly prone to nucleophilic attack. In order to achieve control over sol to gel transformation the alkoxide hydrolysis rate has to be controlled. This is best achieved by using chelating agents such as β-diketones [11, 12]. Chemical modification of metal alkoxide with chelating agents like β-diketones enables reduction of the hydrolytic activity, i.e., the rate of hydrolysis and therefore control of condensation process of reactive metal alkoxides [11, 13–15].

The β-ketoesters, like Eaa, are capable of undergoing keto-enol tautomerism. The reaction is shown in Fig. 1. In pure Eaa the ketonic form predominates, and enolic content is only about 8% [14]. In the presence of Asb the reactive enol form of Eaa substitutes the alkoxy groups of Asb (Fig. 1). A replacement of the reactive alkoxy group with less hydrolysable entity, i.e., the formation of a chelate, strongly shifts keto-enolic equilibrium towards enolic form stabilized by chelation with Asb.

Some key works in the field of chelation of aluminum alkoxides and hydrolysis of obtained chelates are those of Nass and Schmidt [14], Mehrotra [16], Bonhomme-Coury et al. [12], Tadanaga et al. [13], Yamada et al. [17], Le Bihan et al. [18], and Hoebbel et al. [19]. β-diketones such as ethyl acetoacetate and acetyl acetone have been successfully applied to produce nano-alumina powders, alumina thin films [14, 20], alumina fibers [21], alumina aerogels [22, 23], mullite [24] and cordierite [15, 25].

The structure of modified alkoxide affects the structure of gel formed by its hydrolysis. The coordination number of aluminium atoms increases upon introducing chelating agent, which is reflected in hydrolysis process, gel structure and physical properties of the final material.

For this reasons, sol–gel synthesis of CA from Asb and $Ca(NO_3)_2 \times 4H_2O$ have been subjected to investigation. Asb has been chelated with Eaa in various ratios. After hydrolysis, the structure of the prepared gels has been investigated with spectroscopic techniques. The influence of the extent of alkoxide modification on gel formation, structure and thermal evolution of gels has been reported.

2 Experimental

2.1 Synthesis

Precursor materials used to prepare gels were Asb ($Al(O^sBu)_3$, 97%, Aldrich, Great Britain), Eaa ($C_6H_{10}O_3$, 99%, Fluka, Germany) and $Ca(NO_3)_2 \times 4H_2O$ (p.a. assay, Kemika, Croatia). Isopropyl alcohol (C_3H_7OH, 99%, Kemika, Croatia) was used as a solvent as it is experimentally proven to be a good mutual solvent for the Asb-Eaa system [11]. All chemicals were used as received.

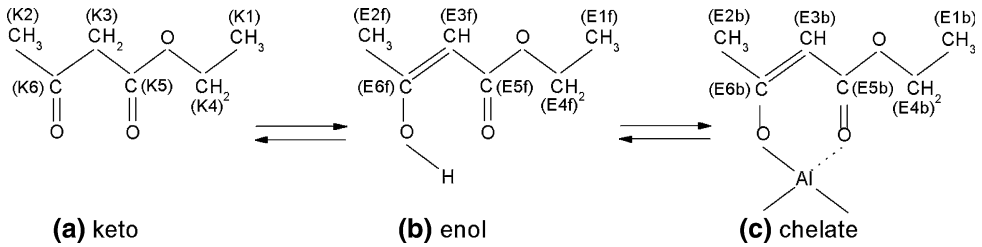

Fig. 1 Keto-enol tautomerism and formation of chelate. Labels are introduced for ^{1}H and ^{13}C NMR resonance peaks description. K-keto, E-enol, f-free, b-bonded to Al

Three gels were prepared, with Eaa/Asb molar ratios of 1/1, 3/2 and 2/1, denoted accordingly. The influence of the amount of the solvent, synthesis duration and the addition of water were examined in preliminary experiments, in order to define optimal synthesis conditions. The increased solvent content prolonged the gel formation without any benefit to gel homogeneity and final phase purity, determined using XRD. Similar was with the prolonged synthesis duration while the addition of water resulted in far less homogeneous gel. Therefore, room temperature, 1 day synthesis and the slowest water addition rate possible, slow hydrolysis with air moisture was applied. An additional sample without calcium nitrate and solvent, having 2/1 Eaa/Asb molar ratio, noted AE2, was additionally prepared in order to clarify some observations noted in the course of investigation.

The Eaa was firstly added to the solvent and then the appropriate amount of Asb was dissolved in solvent/Eaa solution. Asb was added to the solution using syringe to minimize exposure to air humidity. Upon addition of Asb to the Eaa/solvent solution the exothermic process occurs. The appropriate amount of $Ca(NO_3)_2 \times 4H_2O$ was dissolved in solvent separately. Both solutions were stirred for 1 h before the $Ca(NO_3)_2 \times 4H_2O$ solution was added dropwise to the Eaa/Asb solution. The molar ratio of Asb:$Ca(NO_3)_2 \times 4H_2O$:solvent was 2:1:10, and the molar ratio of Eaa:Asb was 1:1, 1.5:1 and 2:1 for samples 1/1, 3/2 and 2/1, respectively. No water was added except for water present in $Ca(NO_3)_2 \times 4H_2O$. Before the addition of $Ca(NO_3)_2 \times 4H_2O$ sample 2/1 was slightly turbid, upon addition of Ca nitrate a clear sol reappeared. The mixture was stirred in a closed reactor for 24 h at room temperature, no precipitation was observed.

The clear sols were poured into a large Petri dish in order to maximize exposure to air moisture and kept at room temperature. After two days the gellation occurred, for the samples 3/2 and 2/1 a completely transparent gel has been obtained. Sample 1/1 yielded a white fragile solid upon hydrolysis. Sample AE2 turned to white sticky solid in <12 h. Drying of the samples for five more days at room temperature enabled the evaporation of solvent and the release of alkoxy groups resulting with a dry product. The obtained samples were subsequently grinded to fine powders and stored. The measurements were done approximately 1 month after the synthesis.

2.2 Characterization

IR spectra of the samples were acquired using the Fourier transform infrared spectrometer Bruker Vertex 70 in ATR (attenuated total reflectance) mode. The samples were pressed on a diamond and the absorbance data were collected between 400 and 4,000 cm^{-1} with spectral resolution of 1 cm^{-1} and 64 scans.

^{1}H and ^{13}C NMR spectra were recorded on high-resolution NMR Spectrometer Bruker Avance 300, operating at 298.64 MHz for ^{1}H resonance and for ^{13}C at 75.10 MHz. The samples were dissolved in C_6H_6-d_6 and measured in 5 mm NMR tubes. The ^{1}H and ^{13}C NMR chemical shift values (δ) are expressed in ppm referred to tetramethylsilane (TMS) as internal standard and coupling constants (J) in Hz.

^{27}Al magic-angle spinning (MAS) NMR spectra were recorded on a 600 MHz Varian NMR system, operating at ^{27}Al Larmor frequency of 156.3 MHz. Sample rotation frequency was 10 kHz, repetition delay between consecutive scans was 1 s and the number of scans was 480. In all spectra, frequency axis in ppm is reported relative to the signal of aluminum nuclei within 1 M solution of $Al(NO_3)_3$. ^{27}Al 3QMAS spectrum was obtained by a z-filtered pulse sequence [26] using a hypercomplex approach. Spectral width and number of increments along the indirectly detected dimension were 20 kHz and 48, respectively.

Mass spectrum was recorded using electrospray ionization technique (ESI) on the Micromass Platform LCZ single quadropole mass spectrometer. Prior to analysis sample was dissolved in acetonitrile. Elemental analyses for carbon and hydrogen were performed on the Perkin Elmer 2400 elemental analyzer.

The crystal phases were identified by powder X-ray diffraction (XRD) using Philips diffractometer PW 1830 with CuKα radiation. Data were collected between 5 and 70° 2θ in a step scan mode with steps of 0.02° and counting time of 2 s.

3 Results

3.1 FTIR spectroscopy

The chelation process was examined using FTIR. Infra red spectra of chelating agent, sol of the sample 3/2 and samples 1/1, 3/2 and 2/1 after hydrolysis are presented in Fig. 2. The assignments of FTIR spectra of Eaa based chelates, described in literature, are often incomplete and sometimes contradictory. Therefore, the assignment of absorption bands has been reevaluated and based primarily on handbook [27], as well as on recent papers [12, 13, 17–19, 28–30].

IR spectrum of Eaa shows bands for ketonic and enolic form. Eaa in ketonic form shows absorption frequencies of C–H stretching vibrations in region 2,980–2,850 cm^{-1}. Band at 2,980 cm^{-1} results from the asymmetrical (as) stretching mode in which two C–H bonds of the methyl group are extending, while the third one is contracting (ν_{as} CH_3). Band at 2,870 cm^{-1} arises from symmetrical (s) stretching (ν_s CH_3) in which all three C–H bonds extend and contract in phase. The asymmetrical stretching (ν_{as} CH_2) and symmetrical stretching (ν_s CH_2) occur at 2,940 and 2,850 cm^{-1}, respectively. Characteristic bands for the ketonic form of Eaa occurs at 1,753–1,718 cm^{-1} due to the C=O stretching vibration of two carbonyl groups (one being slightly shifted due to an inductive effect of esteric oxygen). Spectrum also exhibits bands at 1,475 cm^{-1} (due to asymmetrical bending vibration involves out-of-phase bending of the C–H bonds, δ_{as} CH_3) and 1,369 cm^{-1} (due to symmetrical bending vibration involves in phase bending of the C–H bonds, δ_s CH_3). The scissoring band (δ_s CH_2) in the spectrum occurs at 1,470 cm^{-1}. A series of bands in the region 1,350–1,150 cm^{-1} is characteristic for esters, because of methylene twisting and wagging vibrations. In addition to that, the absorption frequencies of O–C–C stretching, –C–C–O stretching and C–C stretching occur at 1,040, 1,155 and 1,317 cm^{-1}, respectively.

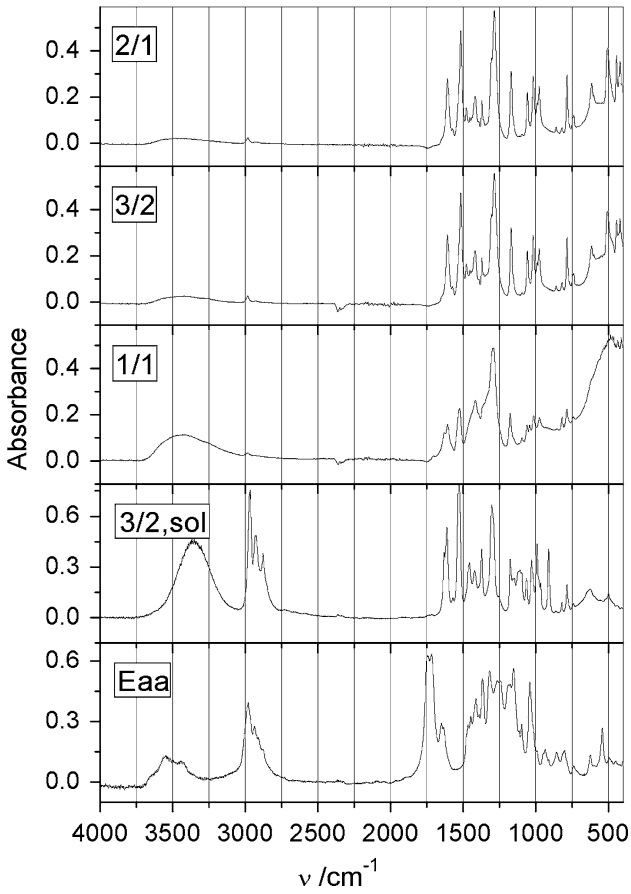

Fig. 2 IR spectra of chelating agent, sol 3/2 and gels 1/1, 3/2 and 2/1

The majority of absorption bands, rising from ketonic form, rise also due to an enolic form. Instead of bands of the ketonic form of Eaa at 1,753–1,718 cm^{-1}, in the spectrum of enolic form characteristic bands are observed at 1,650 cm^{-1} due to hydrogen bonding between the ester C=O and the enolic hydroxyl group, as well as absorption frequencies of the alkene bond in conjugation with a carbonyl group at 1,630 cm^{-1}.

The C–H rocking vibration of alkene occurs at 1,415 cm^{-1}. The most characteristic vibrational modes of alkenes are the out of plane C–H bending vibrations between 620 and 940 cm^{-1}.

Therefore, the most characteristic absorption bands in FTIR spectra of ketonic form are at 1,753–1,718 cm^{-1}, while the enolic form is characterized by absorption band at 1,650 and 1,630 cm^{-1}. On the other hand, Eaa in chelate shows characteristic absorption bands at $\sim$1,610 cm^{-1} due to a C–O in enolic form bonded to Al, as well as absorption band at $\sim$1,525 cm^{-1} due to a C–C vibration of six membered ring of the complex.

FTIR spectra presented in Fig. 2 confirm that Eaa, in all samples, i.e., for all Eaa/Asb ratios, reacts completely with Asb forming chelate. Following reaction occurs:

$$Al(O^SBu)_3 + nMeCOCH_2COOEt \rightarrow Al(O^SBu)_{3-n}(MeCOCHCOOEt)_n + n^SBuOH$$

FTIR spectrum of 3/2 sol, beside absorption bands of Eaa in chelate, is characterized by absorption bands of isopropanol. The most pronounced bands are wide band between 3,600 and 3,000 cm^{-1} (OH stretching vibrations), bands between 3,000 and 2,800 cm^{-1} (C–H stretching vibrations), series of bands in range 1,500–1,200 cm^{-1} (CH_3 symmetrical and asymmetrical bending vibrations) and 1,200–1,100 cm^{-1} (C–O stretching vibrations) and single bands at $\sim$950 cm^{-1} (CH_3 rocking vibrations in isopropyl group) and 820 cm^{-1} (CH_3 rocking vibrations). The major absorption bands due to a NO_3^- are located at

1,305, 1,445 and 1,630 cm^{-1}, mostly overlapped with Eaa bands.

In FTIR spectra of hydrolyzed gels the absorption bands due to a C–H stretching in region 2,980–2,850 cm^{-1} almost disappear, but the characteristic bands of Eaa in chelate still exist. All bands are strong for the sample 2/1, slightly weaker for the sample 3/2, both being similar to spectra of a sol, except for the absence of evaporated propanol solvent. Bands of the sample 1/1 are very weak. The sample 1/1 was indeed prepared with half of the quantity of Eaa compared to sample 2/1 but it still seems that a considerable part of Eaa has been released during hydrolysis. On the other hand, bands due to a hydroxyl groups bonded to alumina [14], which give absorptions around 3,600 cm^{-1}, increase in reverse order, i.e., 2/1 < 3/2 < 1/1. On spectra of the sample 1/1 a broad band around 500 cm^{-1} is present, probably due to a formation of Al–O–Al bonds by condensation process [12].

From the obtained FTIR spectroscopy results it is obvious that hydrolyzed gels still contain Eaa bonded to alkoxide but it seems that, at least for sample 1/1 a part of Eaa from chelate complex is released upon hydrolysis. Regardless of high boiling point of Eaa, some part of released Eaa could evaporate from high surface area powder in the course of gel drying and aging.

3.2 ^{1}H and ^{13}C NMR spectroscopy

^{1}H and ^{13}C NMR spectra of samples 2/1, 3/2 and 1/1 are presented in Figs. 3, 4. Due to advanced hydrolysis the samples were not completely soluble in benzene. Sample 2/1 dissolved almost completely while the sample 1/1 was rather poorly dissolved. It could be assumed that soluble part of sample is predominantly of organic nature, i.e., the chelated moieties, while the unsoluble part of the sample are predominantly of inorganic nature. The nature and amount of the dissolved species are different, depending on the extent of condensation and the amount of organic ligand present. Hydrogen and carbon atoms are labeled according to Fig. 1. Assignments of ^{1}H and ^{13}C NMR spectra were performed on the basis of chemical shifts, signal intensities, magnitude and multiplicity of H–H coupling constants, as well on the basis of literature references [12, 17, 19, 29, 31].

The perusal of ^{1}H NMR spectrum of sample 2/1 clearly showed the presence of three species, chelate, ketonic Eaa and enolic Eaa in which the major compound is chelate (chelate:ketonic Eaa:enolic Eaa = 150:5:1).

The ^{1}H NMR spectrum of sample 2/1 exhibit signals due to a enolic form of Eaa bonded to Al: vinylic proton at 5.32 ppm (E3b), methylene protons (E4b) were found as a multiplet at chemical shifts 4.12–4.22 ppm, methyl protons (E2b) at 1.96 ppm for which the H–H coupling pattern is

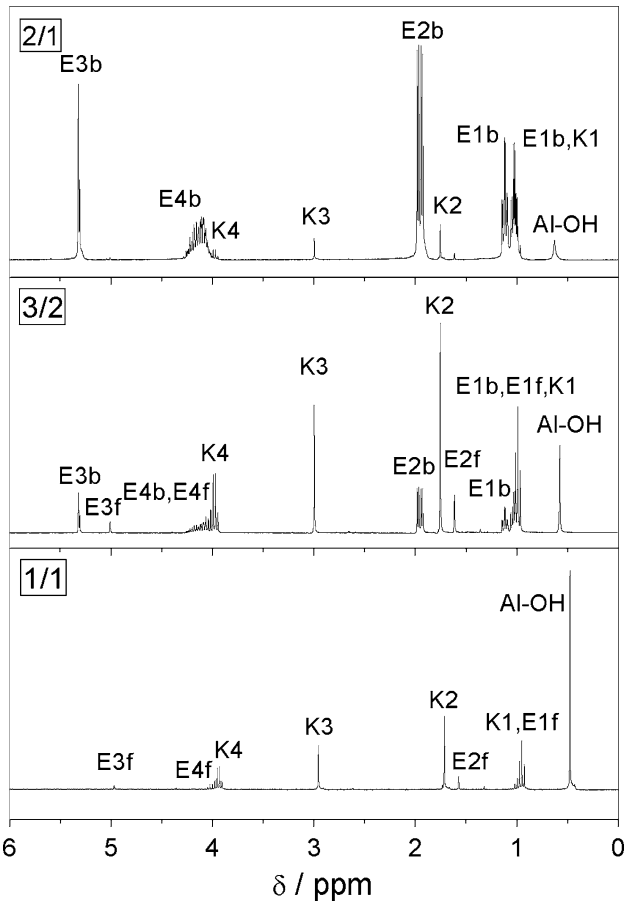

Fig. 3 ^{1}H NMR spectra of samples 1/1, 3/2 and 2/1. Peaks are labeled according to Fig. 1

doublet of doublet (J = 4.89, 11.55 Hz) and methyl protons (E1b) as multiplet at 1.03 and 1.12 ppm. This spectrum also showed minor peaks due to a free Eaa in keto form: singlets for methylene protons at 3.00 ppm (K3) and for methyl protons at 1.76 ppm (K2), a weak signals for methyl (K1) and methylene protons (K4) are overlaped with E1b and E4b. The characteristic signals of the free Eaa in enolic form in this spectrum is the singlet of the vinylic proton (E3f) that occurs at 5.32 ppm and singlet of methyl protons at 1.62 ppm (E2f). Signals for methyl (E1f) and methylene protons (E4f) are overlapped with the peaks of bonded ethylacetoacetate groups (E1b and E4b).

The ^{13}C NMR spectrum of sample 2/1 is in good correlation with ^{1}H NMR showing signals due to an enolic form of Eaa bonded to Al: methyl carbons at 13.9 ppm (E1b) and 22.2 ppm (E2b), methylene carbon at 60.5 ppm (E4b), methyne carbon at 85.4 ppm (E3b) and quaternary carbons at 174.8 ppm (E5b) and 188.4 ppm (E6b). Other peaks due to a free Eaa in keto form are either overlapped or to weak to be visible, except for methyl carbon at 20.5 ppm (K2) and methylene carbon at 49.7 ppm (K3).

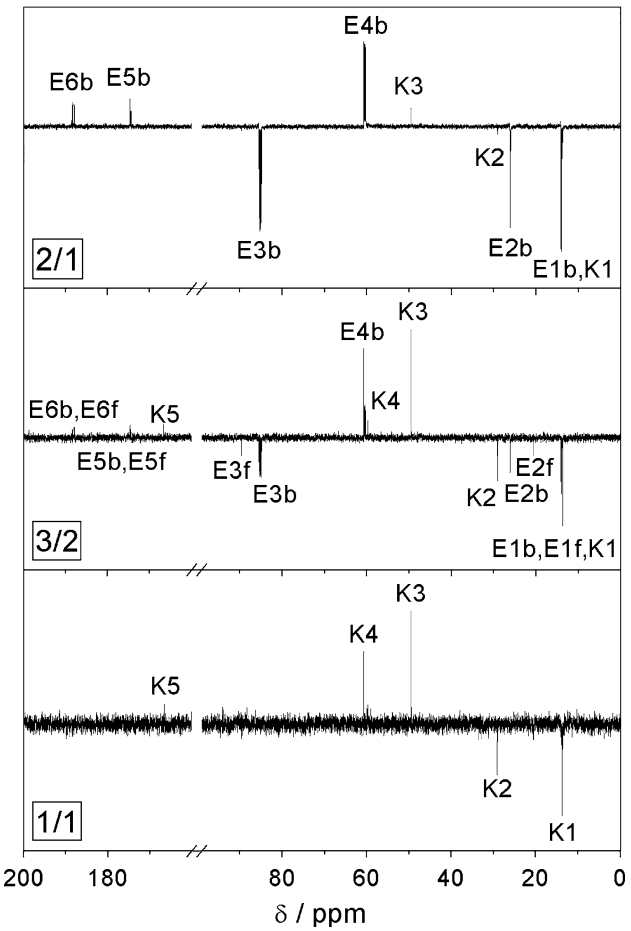

Fig. 4 ^{13}C NMR spectra of samples 1/1, 3/2 and 2/1. Peaks are labeled according to Fig. 1

In the ^{1}H NMR spectrum of sample 3/2 the presence of three species (in ratio ketonic Eaa:chelate:enolic Eaa = 5:4:1) is obvious. The ^{1}H NMR spectrum of sample 3/2 exhibited singlets for methylene protons at 3.00 ppm (K3) and for methyl protons at 1.76 ppm (K2), a triplet ($J = 7.1$ Hz) at chemical shift values of 0.99 ppm for methyl protons (K1) and for methylene protons a quartet ($J = 7.12$ Hz) at 3.98 ppm (K4), that confirmed the presence of Eaa in ketonic form in this sample. The characteristic signals of the enolic form (E3f) and chelate (E3b) in the ^{1}H NMR spectrum of sample 3/2 are the singlets of the vinylic protons, that occur at 5.01 and 5.31 ppm, respectively. The overlapped signals of the methylene protons E4f and E4b were also observed as multiplet at chemical shift values of 4.04–4.16 ppm. Spectrum also showed singlet of methyl protons at 1.62 ppm (E2f) and doublet of doublet ($J = 4.85$, 11.39 Hz) for methyl protons (E2b) at 1.96 ppm. Signals for methyl protons E1b and E1f were found as overlapped multiplet at 1.03–1.15 ppm. The ^{13}C NMR spectrum of 3/2 is in accord with assignments of ^{1}H NMR data.

^{1}H NMR spectrum of sample 1/1 contains signals for each tautomeric form of Eaa in which the ketonic form of Eaa prevails. In the ^{1}H NMR spectrum of sample 1/1 there were characteristic signals of an ethyl ester moiety in ketonic form found: triplet ($J = 7.11$ Hz) at chemical shift values of 0.95 ppm (K1), singlets at 1.71 and 2.96 ppm (K2 and K3) and quartet ($J = 7.12$ Hz) at 3.94 ppm (K4). Furthermore, for enolic form of Eaa minor signals of vinylic proton (E3f) as a singlet at 4.97 ppm, methylene protons E4f (overlapped with K4), methyl protons E1f (overlapped with K1) and E2f as a singlet at 1.57 ppm were also observed. The ^{13}C NMR spectrum of sample 1/1 is in conformity with determination of ^{1}H NMR data.

According to these observations it follows that in sample 2/1 Eaa exist mainly in enolic form bonded to Al. Only a minor part of Eaa is free with ratio between keto and enolic form generally expected for the free Eaa [14] (waist majority of free Eaa in keto form). For the sample 3/2 the ratio between bonded and free Eaa is changed to the benefit of free form. The characteristic peak of Eaa bonded to Al at $\delta_H = 5.32$ (E3b) is weaker, and the characteristic peak of free Eaa in keto form at $\delta_H = 3.00$ (K3) stronger in comparison to sample 2/1. The peaks due to an enolic form of free Eaa are also visible. The ^{13}C NMR spectra corroborate findings of the state of Eaa (bonded or free) in samples. Only resonance peaks due to free forms of Eaa are visible on spectra of sample 1/1. Generally, the quantity of Eaa reduces significantly from sample 2/1, through sample 3/2 to a sample 1/1. The increasing number of scans should be recorded to reveal resonance peaks from sample 2/1 to sample 1/1 which is visible from the increased thickness of baseline. This is consequence of different solubility of the samples, i.e., different organic/inorganic ratio. Therefore, in sample 2/1 stable form of chelate, resistant to hydrolysis exist and the majority of Eaa added during synthesis is still in the sample. The presence of greater amount of chelating ligands, less hydrolysable than alkoxy groups, changes the functionality of the precursor and prevents hydrolysis [14]. Far less Eaa is in sample 3/2, smaller part in chelate and greater as free forms. In the sample 1/1 only traces of Eaa are present being completely in free forms. Such behavior was expected because Eaa bonded to alkoxide reduces the extent of the hydrolysis and condensation reactions of metal alkoxide. The residual alkoxy groups are much more subject to hydrolysis than the chelating Eaa [17] so the samples with more remained alkoxy groups (less chelating agent) are hydrolyzed to a greater extent. A part of Eaa is released upon hydrolysis and exists as a free Eaa. The high amount of chelate found for the sample 2/1 is consistent with the fact that this sample has lower condensation degree, the high condensation degree of 1/1 reduces significantly the amount of this species in benzene solution.

It is important to note that no multiple sets of resonance peaks due to bonded Eaa were recorded. Such spectra would suggest the existence of uneqivalent chelating sites [12]. Structural models proposed for Asb [32], as well for Asb chelated with β-diketones [13, 33] suggest that Asb and chelated Asb exist mostly as trimer possessing different chelation sites. The lack of multiple sets of resonance peaks points out that molecules of chelating agent are bonded to only one site type, i.e., that all molecules of chelating agent that remained bonded after hydrolysis are in equivalent sites.

None of the spectra show resonance peaks due to the *sec*-butoxide groups, free or bonded to Al. Part of *sec*-butoxy groups has been replaced with Eaa in the course of chelation and the remaining *sec*-butoxy groups are released during hydrolysis and evaporated.

The resonance peaks in Fig. 3, at 0.48 ppm (sample 1/1), 0.59 ppm (sample 3/2) and 0.62 ppm (sample 2/1) are probably due to H atoms in hydroxyl groups bonded to Al (H–O–Al) in partially hydrolyzed, still soluble oligomeric units. This claim couldn't be corroborated with literature data but it seems quite logical since the intensity of this peak increases with the decrease of Eaa peaks, i.e., with the progression of hydrolysis process. The additional argument is the increase of FTIR absorption band around 3,600 cm^{-1}, due to a hydroxyl groups bonded to aluminium, in the same manner.

The obtained results corroborate assumption on the predominantly organic nature of soluble part of sample which consist of chelated Al, chelated Al oligomers formed due to hydrolysis and free Eaa.

Curiously, while NMR spectroscopy detected keto form of Eaa in all three samples, FTIR spectroscopy detected no such form. There is a slight possibility that the remaining free Eaa is confined in pores inside the gel and undetectable to ATR FTIR spectroscopy but the samples are powdered and statistically homogeneous, so this is quite unprobable. More probably is that this can be due to effects of the solvent polarity in the NMR experiments influencing the keto-enolic equilibrium. Finally, this could be the consequence of small concentrations of keto form of Eaa in the samples.

From the NMR data it could be concluded that as the molar ratio Eaa/Asb increases, the possibility of hydrolysis and condensation reactions decreases. With the increase of amount of Eaa, the increased number of alkoxy groups is replaced. Since the Eaa groups are much less subject to hydrolysis than alkoxy groups, samples with less remaining alkoxy groups are less hydrolyzed [17].

3.3 XRD of the gels

XRD pattern of the sample 1/1 exhibits two broad peaks which could be ascribed as amorphous phase. On the other hand, samples 3/2 and, especially, 2/1 show diffraction peaks (Fig. 5). Two phases were detected in the samples 3/2 and 2/1. In the sample 3/2 both phases could be ascribed as minor components, but in sample 2/1 one phase is present in considerable quantity. Minor phase is identified as $Ca(NO)_3 \times 4H_2O$ (ICDD-PDF No. 49-1105). We were unable to find other phase in the database. XRD pattern of sample AE2 (sample without calcium) also showed well defined diffraction peaks of this phase (Fig. 5). Le Bihan [18] reports that chelation of Asb with acetylacetone for ratio higher than 1, results in a precipitation of well-defined $Al(acac)_3$ compound. The precipitation of Eaa–Asb complex is reported by Hoebbel et al. [19] but without additional information.

3.4 Solid-state ^{27}Al MAS and 3QMAS NMR spectroscopy

In order to obtain additional information on the structure and on the coordination of aluminum, gels were studied by ^{27}Al MAS NMR spectroscopy. The ^{27}Al MAS NMR spectra of samples 1/1, 3/2, 2/1 and AE2 are shown in

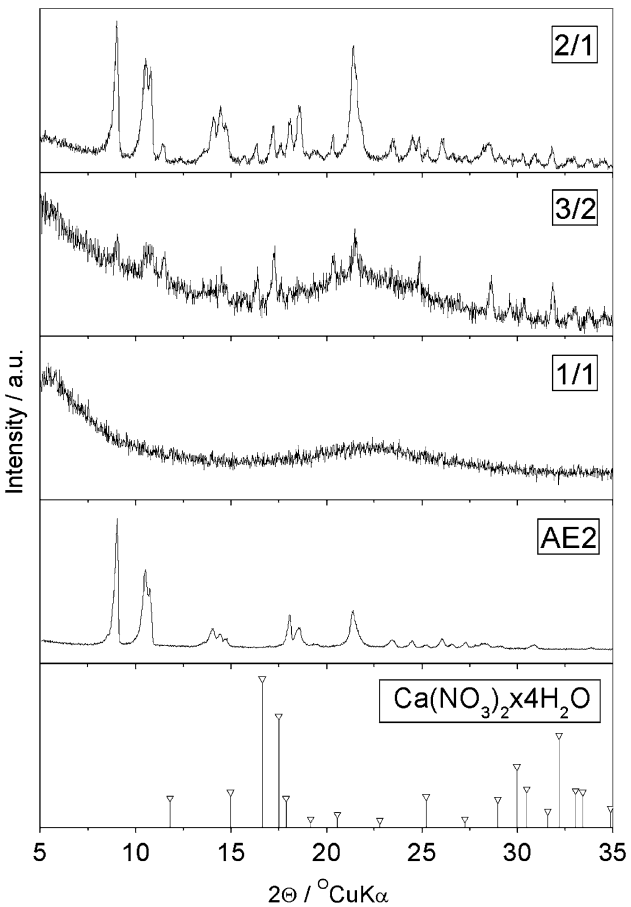

Fig. 5 Powder X-ray diffraction patterns of gels 1/1, 3/2, 2/1 and AE2

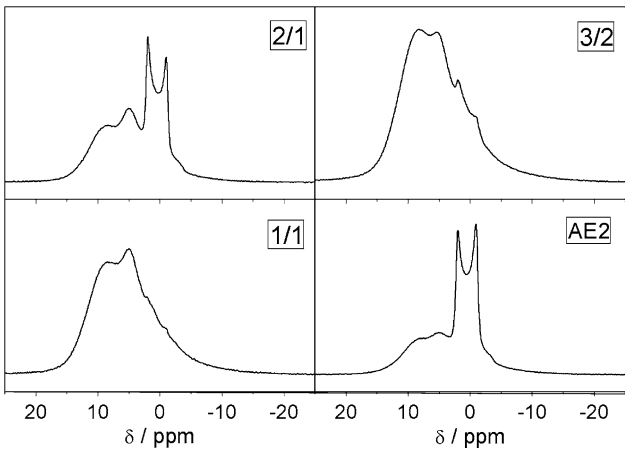

Fig. 6 Solid state ^{27}Al MAS NMR spectra of samples 1/1, 3/2, 2/1 and AE2

Fig. 6. They are composed of several asymmetric contributions that substantially overlap with each other and thus suggest that aluminum atoms occupy several different sites in these samples. Obviously, various kinds of structural units are formed by chelation followed by hydrolysis and condensation.

Resolution of ^{27}Al MAS NMR spectra can be improved by a two-dimensional 3QMAS technique. The spectrum of sample 3/2 is shown in Fig. 7. It exhibits three well-resolved peaks, which can be denoted with A, B and C. The estimated isotropic chemical shifts and quadrupole coupling constants for the corresponding three sites are given in Table 1.

Site A is very well defined and exhibits a typical second-order quadrupolar lineshape with sharp discontinuities. On the other hand, site B and site C are far less defined. Especially the latter one exhibits a wide distribution of chemical shifts and quadrupole coupling constants, which suggests that the surrounding of Al in site C is not uniform throughout the sample. Isotropic shift of Al in site A points out to six-fold coordination, while isotropic shift of Al in site C points out to five-fold coordination. Isotropic shift of Al in site B is in between and indicates either five- or six-fold coordination.

Table 1 Estimation of isotropic chemical shifts and quadrupolar coupling constants of signals A, B and C of a 3QMAS spectrum

Site	δ_{iso}/ppm	C_Q/MHz
A	3.2	3.1
B	6.0	2.0
C	11.2	2.8*

* Very rough estimation, large distribution in δ_{iso} and C_Q

Based on 3QMAS NMR experiment, the ^{27}Al spectra in Fig. 6 could be interpreted as follows: The fraction of Al occupying a well-defined hexacoordinated site A is decreasing from the sample 2/1 over the sample 3/2 to the sample 1/1. The largest fraction of hexacoordinated Al atoms (about 60%) can be found in sample AE2. This sample has the same Eaa/Asb ratio as the sample 2/1.

An MS scan of sample AE2 in range 50–1,000 *m/z* revealed multiple *m/z* signals. Majority of signals are fragments, e.g., $m/z = 285.0896$ which could be assigned to $[Al(Eaa)_2]^+$. Some of the oligomeric fragments we were unable to assign, but the signal (although relatively small) $m/z = 415.1544$ is unambiqously assigned to $[Al(Eaa)_3]H^+$.

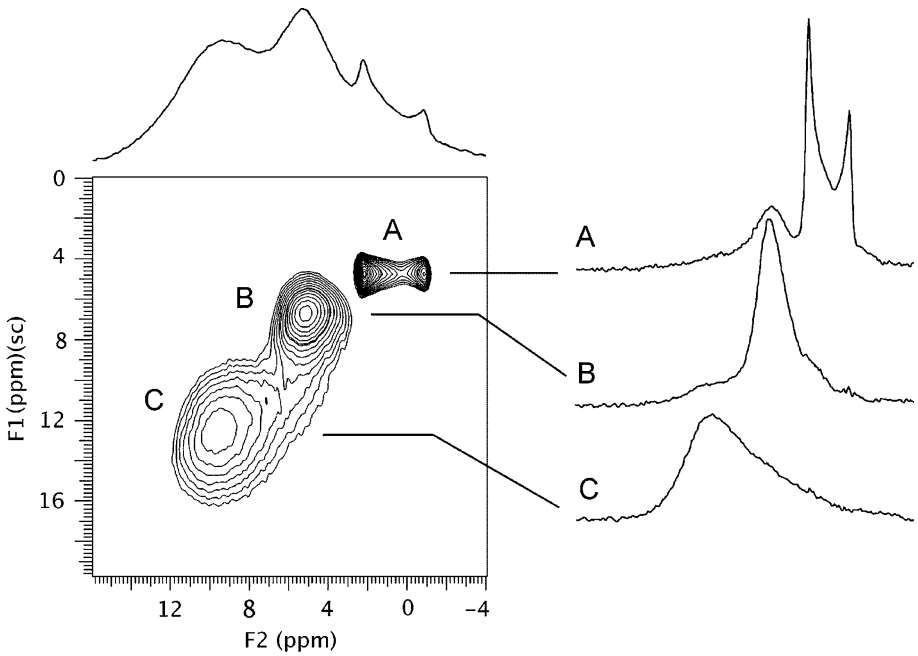

Fig. 7 ^{27}Al (sheared) 3QMAS NMR spectrum of sample 3/2

Chemical analysis of the sample AE2 yielded 46.26% C, 6.59% H and inorganic residue 16.25%. The quantity of carbon remaining in a dried sample AE2 corresponds to quantity of initially added chelating agent fitting ratio Eaa/Al = 2/1. According to chemical analysis the overall stoichiometry of sample AE2 is close to $Al(Eaa)_2OH$ but this data should be interpreted as a mixture of $Al(Eaa)_3$ compound and $Al(Eaa)OH_2$ oligomer. Wengrovious [33] reports that $[Al(OR)(\beta\text{-diketonate})_2]_2$ compounds are unstable and decompose via ligand disproportion to give $Al(\beta\text{-diketonate})_3$ and $[Al(OR)_2(\beta\text{-diketonate})]_2$ products. This disproportionation reaction may in part be due to the steric crowding about octahedral Al centers. Another factor in disproportionation reactions may be the favorable stability of the resulting $Al(\beta\text{-diketonate})_3$ chelates.

Based on samples initial stoichiometry, ^{1}H and ^{13}C NMR spectra of samples 2/1, 3/2 and 1/1, XRD patterns of samples 2/1, 3/2, 1/1 and AE2 and MS results and chemical analysis of the sample AE2, the site A could be assigned to $Al(Eaa)_3$ complex while sites B and C could be assigned to Al sites in polymerized gel. As can be seen for the sample 1/1, where according to ^{1}H and ^{13}C NMR spectra (Figs. 3, 4) only traces of Eaa survived hydrolysis and are not attached to Al but exist in free form, resonance peak at 3.2 ppm is almost invisible (Fig. 6). The same resonance peak increases for sample 3/2 and dominates the spectrum of sample 2/1 (Fig. 6) in which a large amount of Eaa is still attached to Al (Figs. 3, 4). The peak at 3.2 ppm is even more intense in sample AE2 compared to sample 2/1, just as XRD pattern of this sample showed better defined diffraction peaks both being due to a greater quantity of $Al(Eaa)_3$ complex in sample. This is quite expectable because sample AE2 is composed of Asb and Eaa only, without calcium nitrate.

Tadanaga et al. [13] reported that the ^{27}Al NMR spectra of Asb, modified with the Eaa, show peaks due to four-, five- and six coordinated structural units. The higher the Eaa/Asb ratio was, the stronger peak assigned to six-coordinated Al was obtained. At the same time the peaks assigned to four- and five-coordinated Al were much weaker.

Bonhomme et al. [12] noted that the spectrum of Asb chelated with Eaa showed an increase of the coordination of Al atoms in comparison with the spectrum of pure Asb as well as evidence for hexacoordinated, pentacoordinated and tetracoordinated sites. These changes are a consequence of the replacement of monodentate $O^{s}Bu$ ligand by a bidentate Eaa group which leads to an increase of the coordination number.

Tadanaga et al. [13] noted that certain types of six-coordinated structural units are easily hydrolyzed and others are hardly hydrolyzed. They find out that many kinds of condensed six-coordination units, most of which are chelated are present in solution after hydrolysis.

On the basis of presented ^{1}H, ^{13}C NMR, solid-state ^{27}Al MAS NMR and MS data a following path of events could be proposed: In the course of chelation of Asb with Eaa mono-substituted, di-substituted and tri-substituted chelates are formed. According to Kriz et al. [32] Asb is present in solution mainly as linear trimer. As proposed by Tadanaga et al. [13], the formation of mono- and di-substituted chelate does not impair trimeric structure. On the other hand, for the formation of tri-substituted chelate it seems that decomposition of trimer occurs. The ratio between various $Al(O^{s}Bu)_{3-x}(Eaa)_x$ units depends on the amount of Eaa added and it changes to the benefit of tri-substituted units with the increase of the amount of Eaa. On hydrolysis the residual alkoxy groups are attacked (hydrolyzed) first, followed with partial hydrolysis of Eaa groups in mono- and di-substituted chelate. In such manner $[Al(OH)_{3-x}(Eaa)_x]_n$ oligomers are formed. According to Nass and Schmidt [14] the polycondensation takes place to a very limited extent. Tadanaga et al. [13] reported that when Eaa/Asb ratio was more than one, the sols did not form gels during aging for 1,000 h in closed containers and that for Eaa/Asb ratio 1 and 1.5 about 80% of chelating agent remains unhydrolyzed at gellation point. Hoebbel et al. [19] reports that high hydrolytic stability of Eaa complexed Al results in small particle size.

Organic complexing agents are known to have important effect on the hierarchical organization of the gel network [34] by modifying the connectivity of the –Al–O–Al– network. The functionality of the precursor influences the precursor resistance to hydrolysis and oligomer formed later on through hydrolysis and condensation process. The more multi-substituted chelates are formed, the more hydrolysis resistant the precursor is. The tri-substituted chelate is completely resistant to hydrolysis and remains in material unchanged. As a consequence the number of well-defined hexacoordinated Al sites in $Al(Eaa)_3$ increases with the increase of Eaa/Asb ratio while the number of less-defined hexacoordinated and pentacoordinated sites in still partially chelated oligomer increase with the decrease of the same ratio.

3.5 XRD of thermally treated samples

The samples were thermally treated in static air at a heating rate of 10 °C min^{-1} and a firing temperature of 1,000 °C for 2 h. Figure 8 shows XRD patterns for the thermally treated powders. The aluminate samples presented 3 crystal structures, which were identified as CA (ICDD-PDF No. 23-1036), as a major crystalline phase, and CA_2 (ICDD-PDF No. 23-1037) and $C_{12}A_7$ (ICDD-PDF No. 48-1882), as a minor phases. The diffraction maxima of minor phases are slightly greater in sample 2/1 comparing to other two samples.

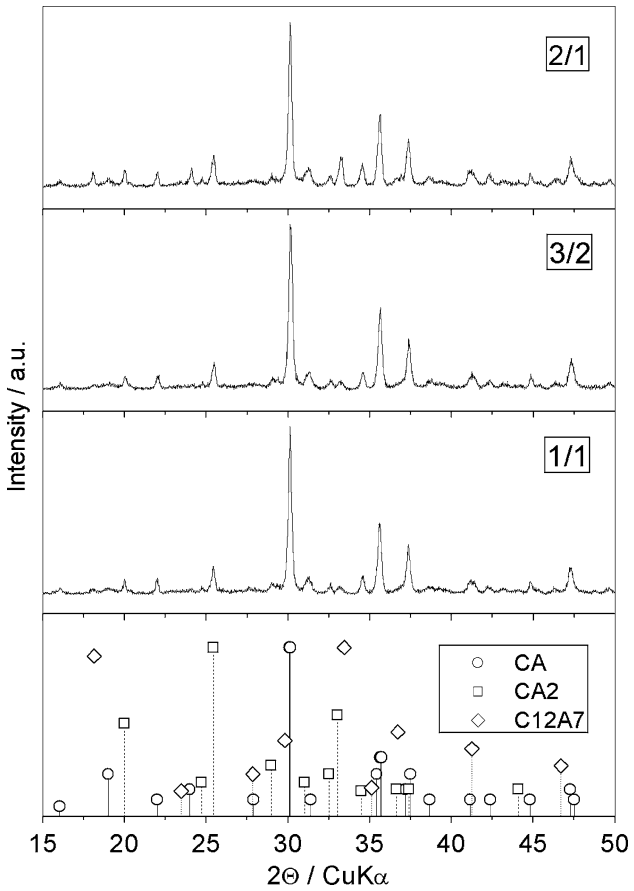

Fig. 8 Powder X-ray diffraction patterns of samples 1/1, 3/2 and 2/1 after heat treatment at 1,000 °C for 2 h

The direct crystallization of calcium aluminate powders obtained by various chemical processing techniques into pure corresponding crystalline phases is rather difficult and rarely reported. This may be due to a: local chemical variations in the composition of the precursors originating from sol segregation, high number of possible compounds in the binary oxide system, inhibition of long-range diffusion of cations at moderate temperatures [2] and more rapid kinetics of other phases [3].

We believe that the primary reason of formation of minor components in our samples is inhomogeneity. The inhomogeneity of the powders arises from Al complexing process. The chelate, as well oligomers, are both free of calcium. Local concentrations of excess aluminium ions, as well of calcium ions (as nitrate) occur, resulting in the formation of aluminium and calcium rich clusters.

A study of the crystallization behavior of prepared calcium aluminate powders is in progress and preliminary results show that prolonged heat treatment or increased heat treatment temperature promote CA crystallization and diminish of the minor phases.

4 Conclusions

The CA gels have been prepared using calcium nitrate tetrahydrate and aluminium *sec*-butoxide. Chemical modification of the Asb precursor has been carried out with ethyl acetoacetate in ratios Eaa/Asb = 1/1, 3/2 and 2/1. The gels composition, structure and thermal evolution were studied using multiple spectroscopic techniques.

Spontaneous gellation has been observed in the sols slowly hydrolyzed by exposing to air moisture. A transparent gels were obtained for the samples with Eaa/Asb = 3/2 and 2/1 ratio.

Eaa reacts completely with Asb forming chelate. However, due to a statistical nature of chelation process various chelate units are formed including trichelated, $Al(Eaa)_3$ units.

The reactivity towards hydrolysis of chelated alkoxide depends on the number of chelating ligands bonded to aluminium. The trichelated units were hardly hydrolysed by the attack of the water molecules in the gellation process, but part of less chelated units undergoes hydrolysis forming oligomeres. *Sec*-butoxy groups were primarily hydrolyzed,

Eaa groups are much less susceptible to hydrolysis thus preventing complete condensation of the alkoxide network, but a part of Eaa groups is also liberated in the course of hydrolysis.

The crystal phase, not described previously, related to $Al(Eaa)_3$ chelate crystallizes in the gels with higher Eaa/Asb ratio.

Hydrolysis led to formation of three kinds of Al coordination sites: six coordinated $Al(Eaa)_3$, and five and six coordinated Al atoms in oligomers. The Eaa/Asb ratio strongly influences the relative ratios between the various coordination states of aluminium atom.

After thermal treatment of the gels at 1,000 °C for 2 h, CA was obtained along with minor CA_2 and $C_{12}A_7$ compounds.

Acknowledgment The financial support of the Ministry of Science, Education and Sports of Republic of Croatia within the framework of the project No. 125-1252970-2981 "Ceramic nanocomposites obtained by sol–gel process" is gratefully acknowledged. The authors would like to thank Dr. E. Mestrovic and I. Bratos, Pliva d.d., Zagreb, Croatia for performing an MS measurement.

References

1. Pati RK, Panda AB, Pramanik P (2002) J Mater Synth Process 10:157. doi:10.1023/A:1023013913102
2. Douy A, Gervais M (2000) J Am Ceram Soc 83:70. doi:10.1111/j.1151-2916.2000.tb01150.x
3. Goktas AA, Weinberg MC (1991) J Am Ceram Soc 74:1066. doi:10.1111/j.1151-2916.1991.tb04344.x

4. Loof J, Svahn F, Jarmar T, Engqvist H, Pameijer CH (2008) Dent Mater 24:653. doi:10.1016/j.dental.2007.06.028
5. Stephan D, Wilhelm P (2004) Z Anorg Allg Chem 630:1477. doi:10.1002/zaac.200400090
6. Gulgun MA, Popoola OO, Kriven WM (1994) J Am Ceram Soc 77:531. doi:10.1111/j.1151-2916.1994.tb07026.x
7. Yi HC, Guigne JY, Moore JJ, Schowengerdt FD, Robinson LA, Manerbino AR (2002) J Mater Sci 37:4537. doi:10.1023/A:1020671626797
8. Uberoi M, Risbud SH (1990) J Am Ceram Soc 73:1768. doi:10.1111/j.1151-2916.1990.tb09829.x
9. Kerns L, Weinberg MC, Myers S, Assink R (1998) J Non-Cryst Solids 232–234:86. doi:10.1016/S0022-3093(98)00376-7
10. Aitasalo T, Holsa J, Jungner H, Lastusaari M, Niittykoski J (2002) Mater Sci 20:15
11. Haridas MM, Goyal N, Bellare JR (1998) Ceram Int 24:415. doi:10.1016/S0272-8842(97)00011-4
12. Bonhomme-Coury L, Babonneau F, Livage J (1994) J Sol-Gel Sci Tech 3:157
13. Tadanaga K, Iwami T, Tohge N, Minami T (1994) J Sol-Gel Sci Tech 3:5
14. Nass R, Schmidt H (1990) J Non-Cryst Solids 121:329. doi:10.1016/0022-3093(90)90153-D
15. Babonneau F, Coury L, Livage J (1990) J Non-Cryst Solids 121:153. doi:10.1016/0022-3093(90)90122-3
16. Mehrotra RC (1988) Pure Appl Chem 60:1349. doi:10.1351/pac198860081349
17. Yamada N, Yoshinaga I, Katayama S (2000) J Sol-Gel Sci Tech 17:123
18. Le Bihan L, Dumeignil F, Payen E (2002) J Sol-Gel Sci Tech 24:113
19. Hoebbel D, Reinert T, Schmidt H, Arpac E (1997) J Sol-Gel Sci Tech 10:115
20. Uchihashi H, Tohge N, Minami T (1989) Ceram Soc Jpn Int Ed 97:398
21. Yogo T, Iwahara LJ (1992) J Mater Sci 27:1499. doi:10.1007/BF00542910
22. Mizushima Y, Hori M (1992) Appl Catal A 88:137. doi:10.1016/0926-860X(92)80211-T
23. Heinrich T, Raether F, Tappert W, Fricke J (1992) J Non-Cryst Solids 145:55. doi:10.1016/S0022-3093(05)80429-6
24. Heinrich T, Raether F, Sprmann O, Fricke J (1991) J Appl Cryst 24:788. doi:10.1107/S0021889890013759
25. Bonhomme-Coury L, Babonneau F, Livage J (1993) Chem Mater 5:323. doi:10.1021/cm00027a015
26. Amoureux JP, Fernandez C, Steuernagel S (1996) J Magn Reson A 123:116. doi:10.1006/jmra.1996.0221
27. Silverstein RM, Webster FX (1998) Spectrometric indetification of organic compounds, 6th edn. Willey, NY, USA
28. Jing C, Zhao X, Zhang Y (2007) Mater Res Bull 42:600. doi:10.1016/j.materresbull.2006.08.005
29. Lafuma A, Chodorowski-Kimmes S, Quinn FX, Sanchez C (2003) Eur J Inorg Chem 2003:331. doi:10.1002/ejic.200390045
30. Krishna Priya G, Padmaja P, Warrier KGK, Damodaran AD, Aruldhas G (1997) J Mater Sci Lett 16:1548. doi:10.1023/A:1018568418302
31. http://webbook.nist.gov
32. Kriz O, Casensky B, Lycka A, Fusek J, Hermanek S (1984) J Magn Reson 60:375
33. Wengrovius JH, Garbauskas MF, Williams EA, Going RC, Donahue PE, Smith JF (1986) J Am Chem Soc 108:982. doi:10.1021/ja00265a024
34. Pierre A, Begag R, Pajonk G (1999) J Mater Sci 34:4937. doi:10.1023/A:1004703504103